Available online at www.sciencedirect.com
ScienceDirect
Ceramics International 36 (2010) 193–197
CERAMICS INTERNATIONAL
www.elsevier.com/locate/ceramint

Upconversion luminescence of high content Er-doped YAG transparent ceramics

Jun Zhou [a,b], Wenxin Zhang [a,b], Jiang Li [a], Benxue Jiang [a], Wenbin Liu [a], Yubai Pan [a,*]

[a] Key Laboratory of Transparent and Opto-functional Advanced Inorganic Materials, Shanghai Institute of Ceramics, Chinese Academy of Sciences, 1295 Ding Xi Road, Shanghai 200050, China
[b] Graduate School of the Chinese Academy of Sciences, 19A Yuquan Road, Beijing 100039, China

Received 4 June 2009; received in revised form 22 June 2009; accepted 10 July 2009
Available online 11 August 2009

Abstract

The various high content Er-doped YAG transparent ceramics with excellent transparency up to nearly 84% at the visible band and the near-infrared band were prepared by the solid-state reaction and the vacuum sintering technique. It is found that the samples exhibit pore-free structures and there are no secondary phases both at the grain boundaries and the inner grains. The average grain size of the Er:YAG ceramics is about 30 μm. The green and red upconversion luminescences in the Er:YAG ceramics pumped by a 980 nm LD were observed. The different upconversion mechanisms depending on Er content in the Er:YAG ceramics and the LD power were also discussed.

Keywords: B. Grain size; C. Optical properties; Er:YAG; Transparent ceramics

1. Introduction

Since the first polycrystalline Nd:YAG ceramic laser pumped by the diode laser excitation system was reported in 1995 [1], highly transparent ceramics research has been speeding up due to its various potential applications in many industrial fields. Many recent studies on the diode-pumped solid-state lasers have focused on polycrystalline ceramic lasers [2–4], and diode-pumped Nd:YAG, Yb:YAG, composite YAG/Nd:YAG/YAG ceramics laser experiments have also been successfully performed [5–8] and other garnet structure ceramics (i.e. TmAG [9]) have been fabricated in our group. Among the rare earth doped YAG materials, high content Er-doped YAG crystal is an important laser material to obtain near 2.94 μm lasers, which is widely utilized by the medical community because of the strong absorption by water in this wavelength range, and 960 nm diode-pumped 1-W continuous-wave 50 at.% Er:YAG crystal 3 μm laser has been performed by Chen et al. [10].

In upconversion schemes, population in an excited state with an energy exceeding the energy of the pump photon may be achieved either by excited state absorption (ESA), or by energy transfer upconversion (ETU), or by photon avalanche (PA), according to the excitation conditions and the specific pump wavelengths used [11], and the drift of upconversion luminescence intensity could reflect the main excitation mode. Therefore, the research on upconversion luminescence and processes in Er-doped YAG ceramics is very significant for the 3 μm high content Er:YAG laser experiment.

2. Experimental procedure

High-purity α-Al_2O_3 ($D_{50} \approx 0.38$ μm, Shanghai Wusong Chemical Co., Ltd., Shanghai, China), Y_2O_3 ($D_{50} \approx 3.35$ μm, Shanghai Yuelong New Materials Co., Ltd., Shanghai, China), and Er_2O_3 ($D_{50} \approx 7.2$ μm, Conghua Jianfeng Rare-Earth Co., Ltd., Guangzhou, China) were used as starting materials. These powders were weighed according to the different stoichiometric ratios of the Er:YAG and milled with Al_2O_3 balls for 12 h with ethanol and tetraethyl orthosilicate. After dried and sieved through 200-mesh screen, the powder mixture was dry-pressed at 5 MPa and then isostatically pressed at

* Corresponding author. Tel.: +86 21 52412820; fax: +86 21 52413903.
E-mail address: ybpan@mail.sic.ac.cn (Y. Pan).

0272-8842/$36.00
doi:10.1016/j.ceramint.2009.07.018

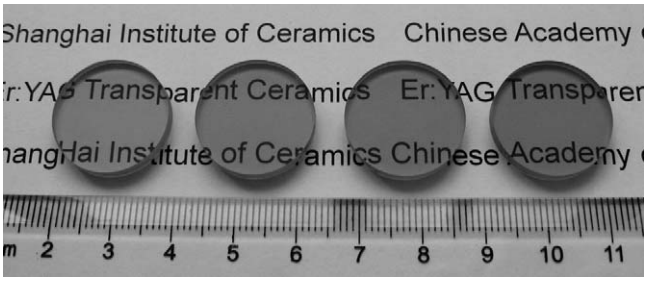

Fig. 1. The mirror-polished Er:YAG ceramics (Er content from the left to the right: 30 at.%, 50 at.%, 70 at.%, and 90 at.%).

250 MPa. The powder compacts were vacuum-sintered at 1780 °C for 20 h under 10^{-3} Pa, then annealed at 1450 °C for 10 h under atmosphere. Before microstructure observation the samples were mirror-polished on both surfaces and thermal-etched at 1500 °C for 2 h.

The microstructures of the samples were observed by the electron probe micro-analyzer (EPMA) (Model JSM-6700, JEOL, Tokyo, Japan). Disk specimens machined to disks (Ø20 mm × 2 mm) and mirror-polished on both surfaces were used to measure optical transmittance (Model U-2800 Spectrophotometer, Hitachi, Tokyo, Japan). For measuring the upconversion fluorescence spectra (Fluorolog-3, Jobin Yvon, Paris, France), the specimens were excited with a 980 nm laser diode (LD).

3. Results and discussion

Fig. 1 shows the photographs of the mirror-polished Er:YAG ceramics with the thickness of 3 mm. All the specimens are deep pink due to the light absorption of Er^{3+} at the visible band (shown in Fig. 3). According to the EPMA photographs shown in Fig. 2, it is found that the specimens are very compact and almost without pores. There are no secondary phases observed both at the grain boundaries and the inner grains. The average grain size of the Er:YAG ceramics is about 30 μm. Depending on the poreless microstructure, the highly Er-doped YAG ceramics possess excellent transparency up to nearly 84% at the visible band and the near-infrared band, as shown in Fig. 3. With the increase of the Er^{3+} content, the absorption peaks are enlarged and amplified comparatively. In this case the absorption saturation will be achieved easier.

The upconversion process mechanism (shown in Fig. 4) of the Er-doped materials has been studied [12]. The atoms at the ground state $^4I_{15/2}$ can be excited to $^4I_{11/2}$ pumped by the LD through the ground state absorption (GSA), then through ESA: $^4I_{11/2} \rightarrow {}^4F_{7/2}$ and ET: $^4I_{11/2} \rightarrow {}^4I_{15/2}$, $^4I_{11/2} \rightarrow {}^4F_{7/2}$, followed by fast cascading relaxation from $^4F_{7/2}$ to the $^2H_{11/2}/^4S_{3/2}$ states, and the green light appears through $^2H_{11/2}/^4S_{3/2} \rightarrow {}^4I_{15/2}$. The red light emission process is firstly GSA: $^4I_{15/2} \rightarrow {}^4I_{11/2}$, followed by the fast cascading relaxation to $^4I_{13/2}$, and then ET: $^4I_{11/2} \rightarrow {}^4I_{15/2}$, $^4I_{13/2} \rightarrow {}^4F_{9/2}$, and finally $^4F_{9/2} \rightarrow {}^4I_{15/2}$.

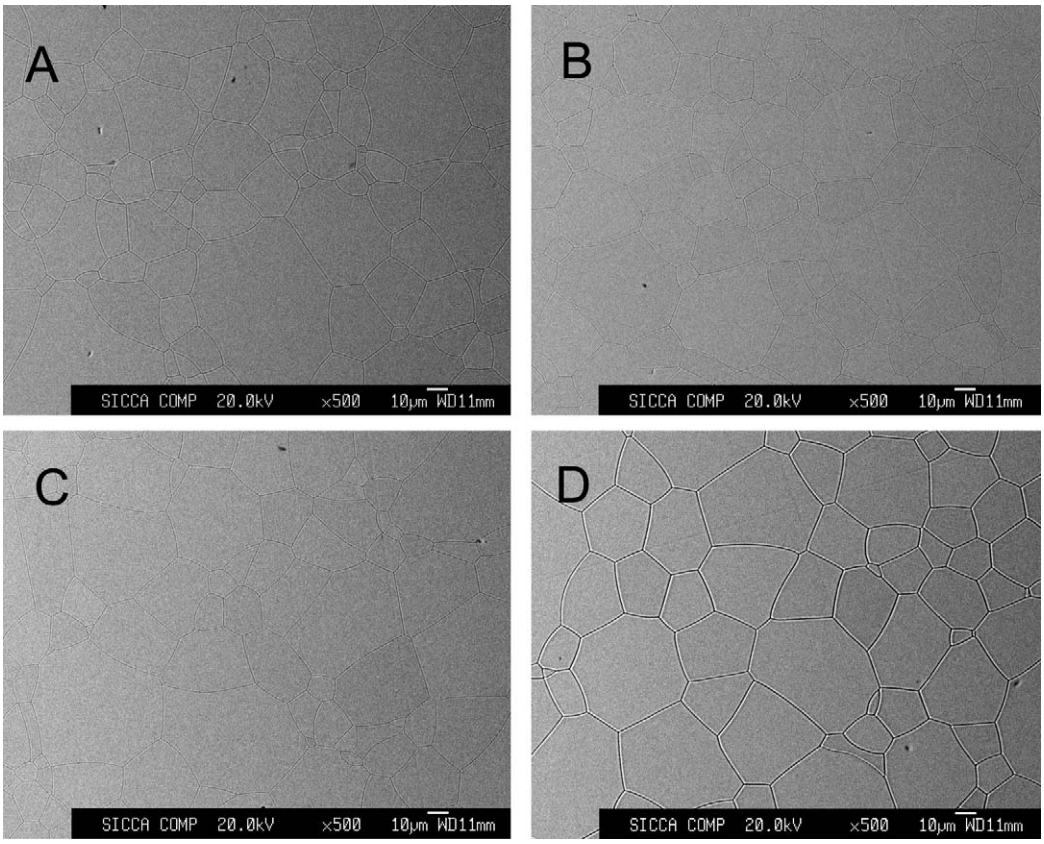

Fig. 2. The EPMA photograph of the Er:YAG ceramics (Er content from A to D: 30 at.%, 50 at.%, 70 at.%, and 90 at.%).

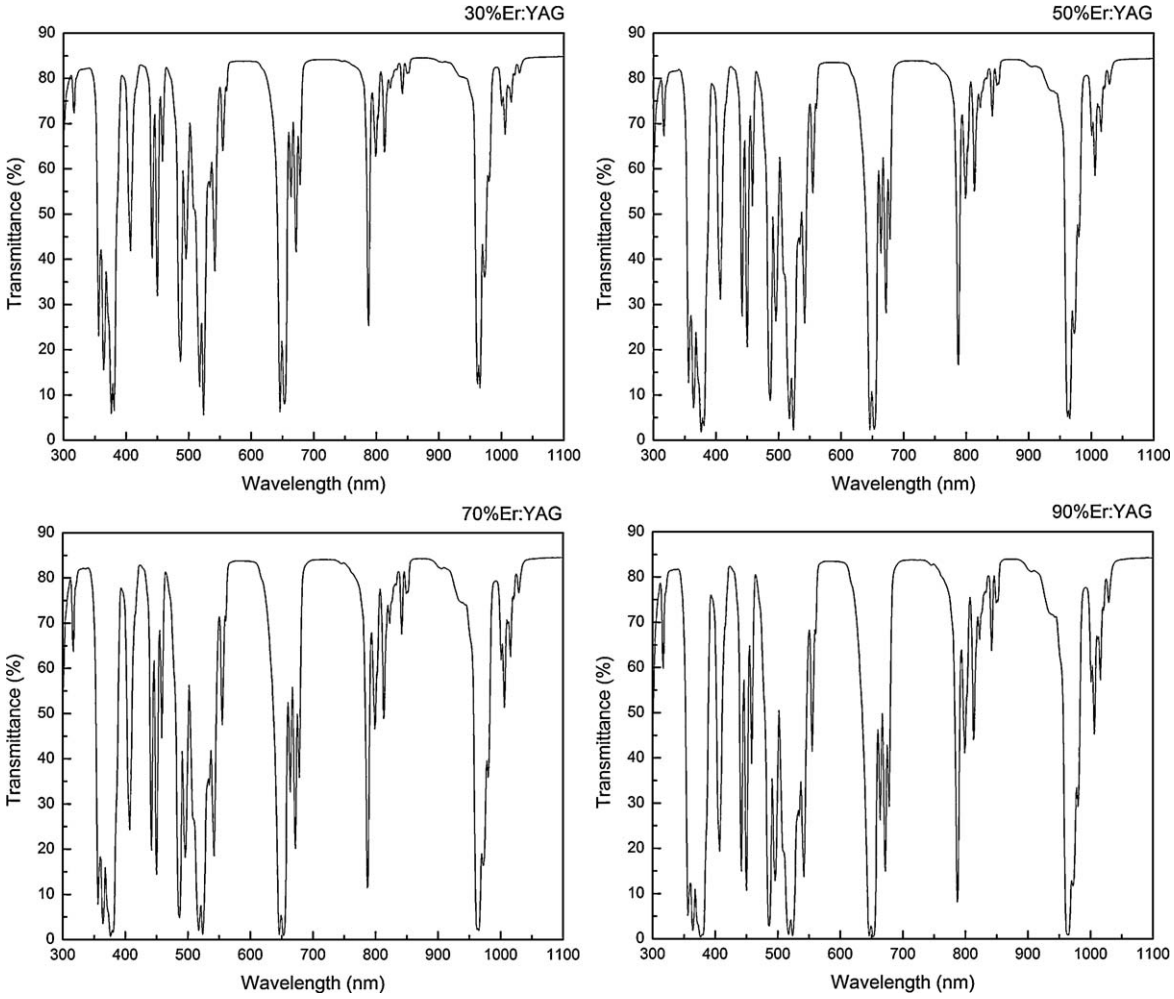

Fig. 3. The optical transmittance spectra of the Er:YAG ceramics.

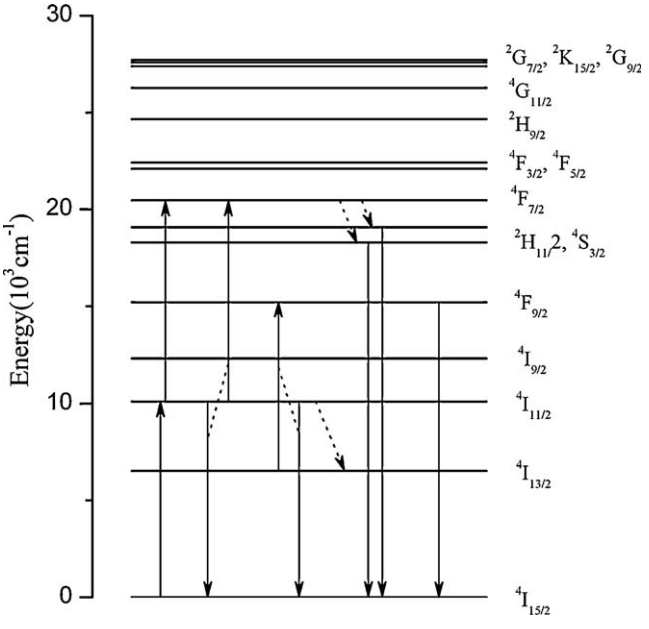

Fig. 4. The upconversion processes in the Er:YAG ceramics excited at 980 nm.

Fig. 5 shows the upconversion spectra of the Er-doped YAG ceramics with different Er content at the room temperature. The electric current of the 980 nm LD pump is 1.35 A corresponding to 500 mW LD power. The similar green (centered at 560 nm) and red (centered at 679 nm) emissions were observed, which originate from the radiative transition of $^2H_{11/2}/^4S_{3/2} \rightarrow {}^4I_{15/2}$ and $^4F_{9/2} \rightarrow {}^4I_{15/2}$, respectively. And it can be found that the red light intensity of the 30 at.% Er:YAG ceramic is the highest among the four samples, and the green light intensity of the 50 at.% Er:YAG ceramic is the highest. Both lights intensities decline fast in the 70 at.% Er:YAG and the 90 at.% Er:YAG ceramics. Fig. 6 shows the dependence of absorption coefficient on Er content in the Er:YAG ceramics. The absorption coefficients of the three kinds of lights (560 nm, 679 nm, and 980 nm) all increase proportionally to Er content with different slopes (980 nm > 679 nm > 560 nm). The luminescence quenchings occur due to the absorption duration of 980 nm laser excitation and the high self-absorption at 560 nm and 679 nm. With the increase of Er content, the luminescence quenching of the red light emerges earlier than that of the

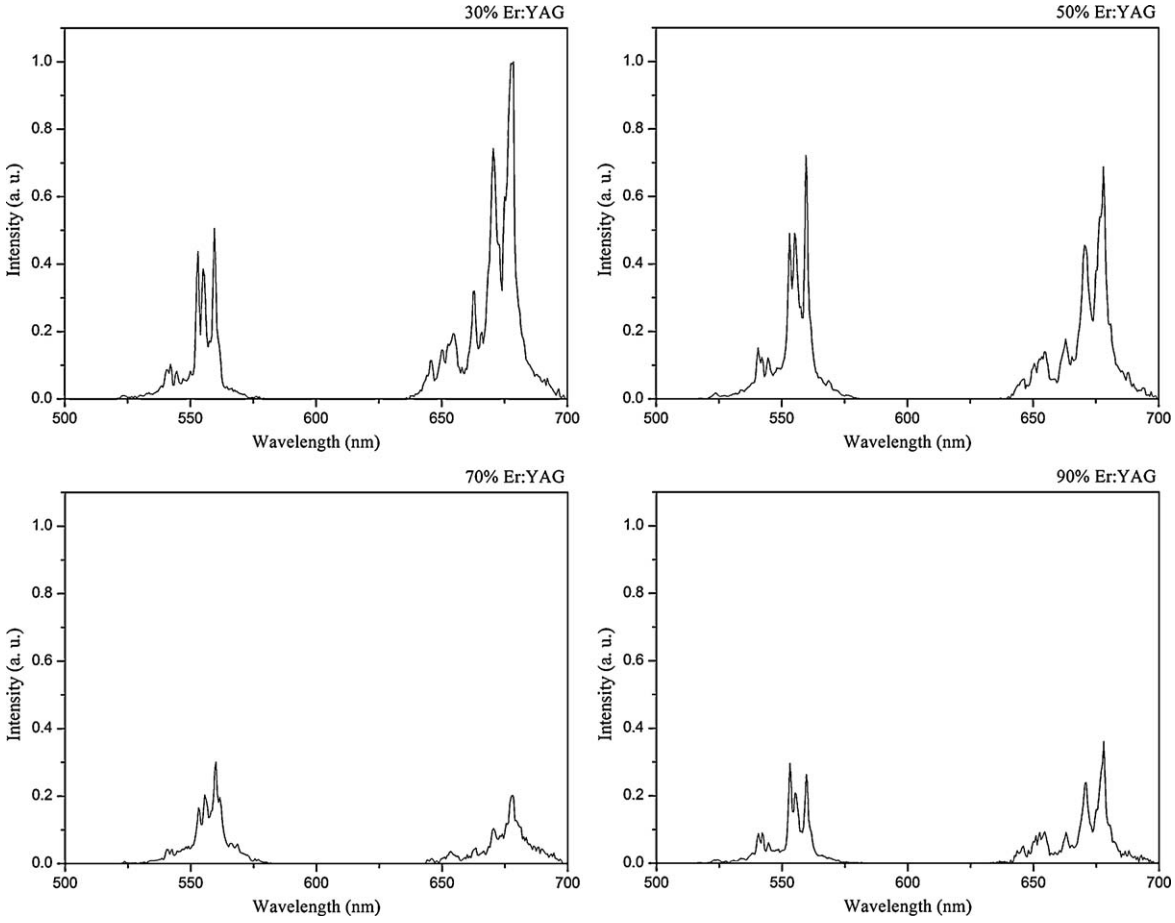

Fig. 5. The room temperature upconversion spectra of the Er:YAG ceramics excited at 980 nm.

green light because of the higher self-absorption coefficient and the heavier slope.

Fig. 7 reveals that the upconversion luminescence intensities increase proportionally along with the increase of the electric current of the 980 nm LD since the electric current and the power of the LD have a linear relation. The slopes (n), calculated by linearly fitting the upconversion luminescence intensity as a function of the LD power, indicates that two photons absorption process are involved in the upconversion mechanism (n = 1.44, 1.43 for the $^4F_{9/2} \rightarrow {}^4I_{15/2}$ transition; n = 1.72, 1.79 for the $^2H_{11/2}/{}^4S_{3/2} \rightarrow {}^4I_{15/2}$ transition), and the slopes are lower than those in low-content (<2 at.%) Er upconversion process ($n = 1.5 \pm 0.1$ for the $^4F_{9/2} \rightarrow {}^4I_{15/2}$ transition; $n = 1.9 \pm 0.1$ for the $^2H_{11/2}/{}^4S_{3/2} \rightarrow {}^4I_{15/2}$ transition) [13]. This may be mainly due to the absorption saturation effect of high-concentration Er^{3+}. According to the upconversion process above, after atoms are excited to

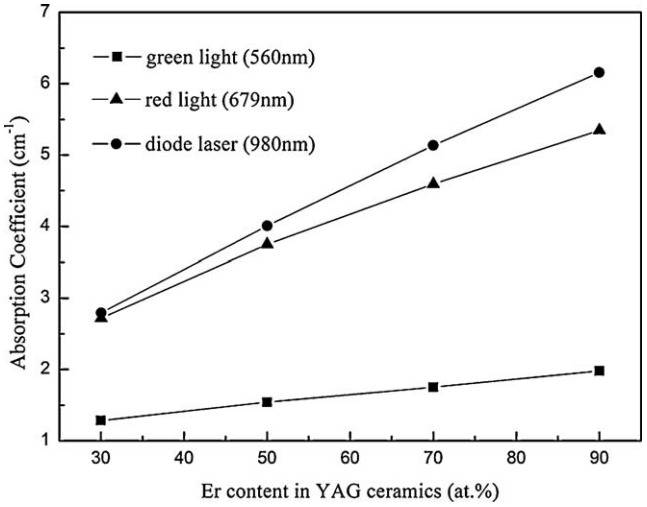

Fig. 6. The dependence of absorption coefficient on Er content in the Er:YAG ceramics.

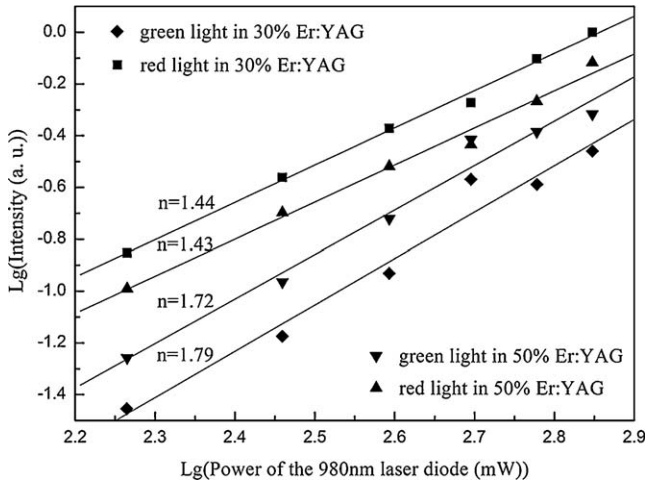

Fig. 7. The intensity dependence of pump power of the 980 nm LD.

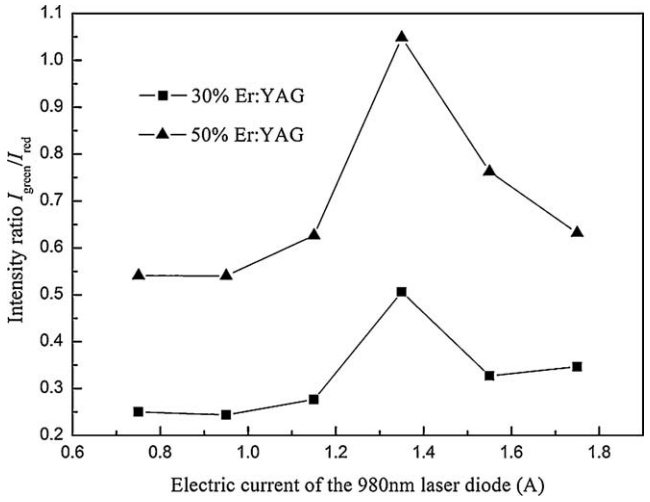

Fig. 8. The dependence of the intensity ratio I_{green}/I_{red} on electric current of the LD.

$^4I_{11/2}$, three possible moves take place: (a) ESA: $^4I_{11/2} \rightarrow {}^4F_{7/2}$; (b) ET: $^4I_{11/2} \rightarrow {}^4I_{15/2}$, $^4I_{11/2} \rightarrow {}^4F_{7/2}$; (c) $^4I_{11/2} \rightarrow {}^4I_{13/2}$. Apparently the first move is more efficient than the second move to emit the green light and invalid to produce the red light, and the third move is the only efficient way to issue the red light and invalid to release the green light. Therefore, the upconversion intensity ratio (I_{green}/I_{red}) could reveal the connection of the three moves. At first, the intensity ratios increase with the electric current of the LD implying ESA ($^4I_{11/2} \rightarrow {}^4F_{7/2}$) and ET ($^4I_{11/2} \rightarrow {}^4I_{15/2}$, $^4I_{11/2} \rightarrow {}^4F_{7/2}$) begin to be dominant among the three possible moves, and achieve the peak at 1.35 A, then begins to decline suggesting the following multiphonon non-irradiative relaxation greatly intensifies: $^4I_{11/2} \rightarrow {}^4I_{13/2}$ and $^4S_{3/2} \rightarrow {}^4F_{9/2}$ according to Fig. 7 and Fig. 8. And the non-irradiative relaxation will bring great heat when the sample is pumped by high power, therefore the sample should be well cooled during the 3 μm Er:YAG ceramic laser experiment.

Additionally, this variation trends of the intensity ratio (I_{green}/I_{red}) seem similar between the 30 at.% Er:YAG and the 50 at.% Er:YAG ceramics. However, the intensity ratio is apparently much larger in the 50 at.% Er:YAG ceramic than that in the 30 at.% Er:YAG ceramic at each power level of the LD, which suggests that the multiphonon non-irradiative relaxation decreases and the incidence of ESA ($^4I_{11/2} \rightarrow {}^4F_{7/2}$) and ET ($^4I_{11/2} \rightarrow {}^4I_{15/2}$, $^4I_{11/2} \rightarrow {}^4F_{7/2}$) are enhanced in the 50 at.% Er:YAG ceramic, compared to the 30 at.% Er^{3+} content. Therefore, the 50 at.% Er:YAG ceramic will be more suitable to be applied during 3 μm laser experiment than the 30 at.% Er:YAG ceramic.

4. Conclusions

In this study, the various high content Er-doped YAG ceramics with excellent transparencies up to nearly 84% at the visible band and the near-infrared band were prepared. The EPMA photograph shows that the specimen is very compact and with no pores. There are no secondary phases observed both at the grain boundaries and the inner grains. The average grain size of the Er:YAG ceramics is about 30 μm.

The green and red upconversion luminescences in the Er:YAG ceramics pumped by 980 nm LD were observed. And the luminescence quenchings of the upconversion emissions were observed. With the increase of the LD power, the ESA process ($^4I_{11/2} \rightarrow {}^4F_{7/2}$) and ET process ($^4I_{11/2} \rightarrow {}^4I_{15/2}$, $^4I_{11/2} \rightarrow {}^4F_{7/2}$) become dominant at lower power of the LD. After the intensity ratio (I_{green}/I_{red}) achieves the peak at 500 mW, the multiphonon non-irradiative relaxation ($^4I_{11/2} \rightarrow {}^4I_{13/2}$ and $^4S_{3/2} \rightarrow {}^4F_{9/2}$) is greatly intensifies with the increase of the LD power. The multiphonon non-irradiative relaxation decreases and the incidence of ESA ($^4I_{11/2} \rightarrow {}^4F_{7/2}$) and ET ($^4I_{11/2} \rightarrow {}^4I_{15/2}$, $^4I_{11/2} \rightarrow {}^4F_{7/2}$) are enhanced in the 50 at.% Er:YAG ceramic, compared to the 30 at.% Er^{3+} content. Therefore, the 50 at.% Er:YAG ceramic will be more suitable to be applied during 3 μm laser experiment than the 30 at.% Er:YAG ceramic.

Acknowledgments

This work was supported by the 863 project (No. AA03Z523) and the Major Basic Research Programs of Shanghai (No. 07DJ14001). And I really appreciate the encouragement and great help from Academician of CAS, Prof. Jingkun Guo and Prof. Liping Huang.

References

[1] A. Ikesue, T. Kinoshita, K. Kamata, K. Yoshida, Fabrication and optical properties of high-performance polycrystalline Nd:YAG ceramics for solid-state lasers, J. Am. Ceram. Soc. 78 (4) (1995) 1033–1040.
[2] T. Yanagitani, H. Yagi, M. Ichikawa, Japanese patent 10-101333, 1998.
[3] J. Lu, M. Prahu, J. Xu, K. Ueda, H. Yagi, T. Yanagitani, A.A. Kaminskii, Highly efficient 2% Nd:yttrium aluminum garnet ceramic laser, Appl. Phys. Lett. 77 (23) (2000) 3707–3709.
[4] J. Lu, T. Murai, K. Takaichi, T. Uematsu, K. Misiwa, M. Prabhu, J. Xu, K. Ueda, H. Yagi, T. Yanagitani, A.A. Kaminskii, 72 W Nd:$Y_3Al_5O_{12}$ ceramic laser, Appl. Phys. Lett. 78 (23) (2001) 3586–3588.
[5] Y. Wu, J. Li, Y. Pan, Q. Liu, J. Guo, B. Jiang, J. Xu, Diode-pumped passively Q-switched Nd:YAG ceramic laser with a Cr:YAG crystal saturable absorber, J. Am. Ceram. Soc. 90 (5) (2007) 1629–1631.
[6] Y. Wu, J. Li, Y. Pan, J. Guo, B. Jiang, Y. Xu, J. Xu, Diode pumped Yb:YAG ceramic laser, J. Am. Ceram. Soc. 90 (10) (2007) 3334–3337.
[7] J. Li, Y. Wu, Y. Pan, W. Liu, L. Huang, J. Guo, Fabrication, microstructure and properties of highly transparent Nd-YAG laser ceramics, Opt. Mater. 31 (1) (2008) 6–17.
[8] J. Li, Y. Wu, Y. Pan, W. Liu, L. Huang, J. Guo, Laminar structured YAG/Nd:YAG/YAG transparent ceramics for solid-state lasers, Int. J. Appl. Ceram. Technol. 5 (4) (2008) 360–364.
[9] W.-X. Zhang, et al., Fabrication and properties of highly transparent $Tm_3Al_5O_{12}$ (TmAG) ceramics, Ceram. Int. (2009), doi:10.1016/j.ceramint.2009.03.039.
[10] D. Chen, C.L. Fincher, T.S. Rose, F.L. Vernon, R.A. Fields, Diode-pumped 1-W continuous-wave Er:YAG 3-μm laser, Opt. Lett. 24 (6) (1999) 385–387.
[11] H.L. Xu, S. Kröll, Upconversion dynamics in Er^{3+}-doped YAG, J. Lumin. 111 (3) (2005) 191–198.
[12] D. Matsuura, Red, green, and blue upconversion luminescence of trivalent-rare-earth ion-doped Y_2O_3 nanocrystals, Appl. Phys. Lett. 81 (24) (2002) 4526–4528.
[13] R.R. Gonçalves, G. Carturan, L. Zampedri, M. Ferrari, A. Chiasera, M. Montagna, G.C. Righini, S. Pelli, S.J.L. Ribeiro, Y. Messaddeq, Infrared-to-visible CW frequency upconversion in erbium activated silica–hafnia waveguides prepared by sol–gel route, J. Non-Cryst. Solids 322 (1–3) (2003) 306–310.